Table I. Photochemical and Photophysical Data for Cyanine Borates

solvent	cyanine lifetime,[a] ps; $[\phi_{fl}]$[b]				k_{et},[d] 10^{10} s^{-1}	
	PF$_6^-$	(C$_6$F$_5$)$_4$B$^-$	(TRPPh)$_4$B$^-$	(C$_6$H$_{11}$Ph)$_4$B$^-$	(C$_6$H$_{11}$Ph)$_4$B$^-$	(TRPPh)$_4$B$^-$
toluene	300; [0.048]	350; [0.05]	490; [0.04]	13;[c] [0.002]	7.1	<0.20
benzene	250; [0.047]	340; [0.05]	520; [0.05]	28;[c] [0.005]	2.6	<0.20
p-xylene	350; [0.066]	410; [0.06]	400; [0.03]	8;[c] [0.001]	13	<0.25
tetralin	435; [0.066]	580; [0.11]	670; [0.04]	6;[c] [0.001]	20	<0.15
p-cymene	e; [e]	520; [0.11]	520; [0.02]	13;[c] [0.003]	7.5	<0.20

[a] Determined by monitoring the rate of ground state absorption recovery or excited state absorption decay following laser excitation. Standard deviations from independent measurements are ±20 ps. [b] Quantum yield of fluorescence determined by excitation at 532 nm for PF$_6^-$ salts and 526 nm for the others. [c] The lifetime of the excited cyanine is too short to measure with an 18-ps laser pulse. These values were computed from the fluorescence yields and the assumption that the radiative and nonradiative rates are the same as for the (C$_6$H$_5$)$_4$B$^-$ salt. [d] Rate constant for electron transfer calculated from the ratio of fluorescence efficiencies of Cy$^+$[(C$_6$F$_5$)$_4$B$^-$] and Cy$^+$[(C$_6$H$_{11}$Ph)$_4$B$^-$] and the lifetime of Cy$^+$[(C$_6$F$_5$)$_4$B$^-$] as described in ref 8. [e] The solubility is too low for accurate measurement of the lifetime and fluorescence yield.

The decrease in fluorescence efficiency and lifetime for Cy$^+$[(C$_6$H$_{11}$Ph)$_4$B$^-$] (borate E_{OX} = 1.14 V vs SCE) compared with those for the perfluorophenyl borate is attributed to electron transfer from the borate to the excited cyanine in accord with observations in related systems.[10,11] Obviously, electron transfer in [(Cy$^+$)*[1](TRPPh)$_4$B$^-$] is inhibited by the change in the substituent on the phenyl groups of the borate from a cyclohexyl to a triptycenyl group. Since this change will have little effect on E_{OX} of the borate, the inhibition of electron transfer must have a steric origin.

The formation of the mono-cis isomer from irradiation of cyanine dyes is generally solvent dependent.[13] We investigated the isomerization of the cyanine borates described in Chart I to probe the microscopic environment of the medium surrounding the cyanine dye. The absorption due to the mono-cis isomer 100 ns after irradiation of the cyanine ion pair in benzene solution (532 nm, 25 ns, 20 mJ) is readily apparent when the anion is [(C$_6$F$_5$)$_4$B$^-$] or PF$_6^-$, but is completely absent for the [(C$_6$H$_{11}$Ph)$_4$B$^-$] and [(TRPPh)$_4$B$^-$] salts. Inhibition of isomer formation for the [(C$_6$H$_{11}$Ph)$_4$B]$^-$ salt is easily explained since rapid electron transfer competes with bond rotation in the excited singlet state of this compound. Surprisingly, both electron transfer and bond rotation are inhibited in [(Cy$^+$)*[1](TRPPh)$_4$B$^-$].

The structures of these salts shown in Figure 1 were computed using PCMODEL.[15] The calculations indicate that energy minimization requires striking a balance between the strong electrostatic attraction of the oppositely charged ions and steric repulsion. For [Cy$^+$(TRPPh)$_4$B$^-$], movement of the phenyltriptycenyl groups away from the symmetrical structure of the free ion opens a cavity that accommodates penetration by the cyanine cation. In this ion pair the central methylene chain and the heteroaryl groups of the cyanine are encased in the borate. For the smaller Cy$^+$[(C$_6$F$_5$)$_4$B$^-$], the cyanine cation does not penetrate the interior of the borate anion significantly. The chemical and physical properties of this salt are consistent with the contact ion pair structure depicted in Figure 1. Further experiments are required to test the validity of these predictions, which provide, at least, a guide to selection of additional structures.

When the cyanine is within the anion, as in [Cy$^+$(TRPPh)$_4$B$^-$], it cannot rotate to form the mono-cis isomer without cooperative motions in the borate. For the smaller borates, cyanine bond rotation remains operational and the singlet lifetime shows a solvent dependence since formation of the mono-cis isomer requires movement of solvent molecules. The magnitude of k_{et} similarly is strongly dependent on the structural details of the penetrated ion pair since it is much smaller for [Cy$^+$(TRPPh)$_4$B$^-$] than it is for [Cy$^+$(C$_6$H$_{11}$Ph)$_4$B$^-$]. Clearly, penetrated cyanine borate

ion pairs have unique, experimentally observable properties that depend on the structural details.


Distinction of Symmetric Lithium Dialkylamide Dimers from Higher Oligomers by Inverse-Detected ^{15}N Homonuclear Zero-Quantum NMR Spectroscopy

James H. Gilchrist* and David B. Collum*

*Department of Chemistry, Baker Laboratory
Cornell University, Ithaca, New York 14853-1301*

^{6}Li and ^{15}N NMR spectroscopy have played a prominent role in the characterization of solvation, aggregation, and mixed aggregation equilibria of lithium dialkylamides.[1-8] It has been suggested that a range of lithium amide cyclic oligomers can exist in hydrocarbon solutions, but that only cyclic dimers are observable in donor solvents.[9] Despite mounting indirect spectroscopic,[2-5] kinetic,[7,10] and theoretical[9,11,12] evidence in support of this model, however, the high symmetry of the more synthetically important lithium dialkylamides has precluded a direct distinction of cyclic dimers (**1**) from other cyclic oligomers (e.g., trimer **2**). We report

1   **2**   **3**
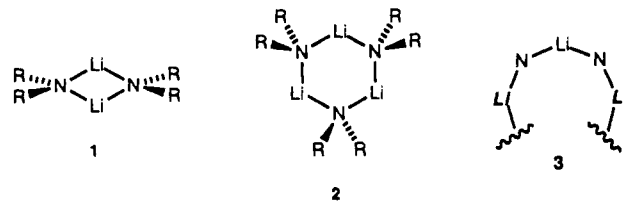
herein a simple NMR experiment in which indirectly detected homonuclear zero-quantum coherence[13] unambiguously differ-

$\tau = 1/4J_{N,Li}$

Figure 1. Pulse sequence used to measure ^{6}Li-detected ^{15}N zero-quantum NMR spectra. Zero-quantum coherence was selected by cycling the third ^{15}N pulse through four phases (0°, 90°, 180°, 270°) and adding the resulting free induction decays.
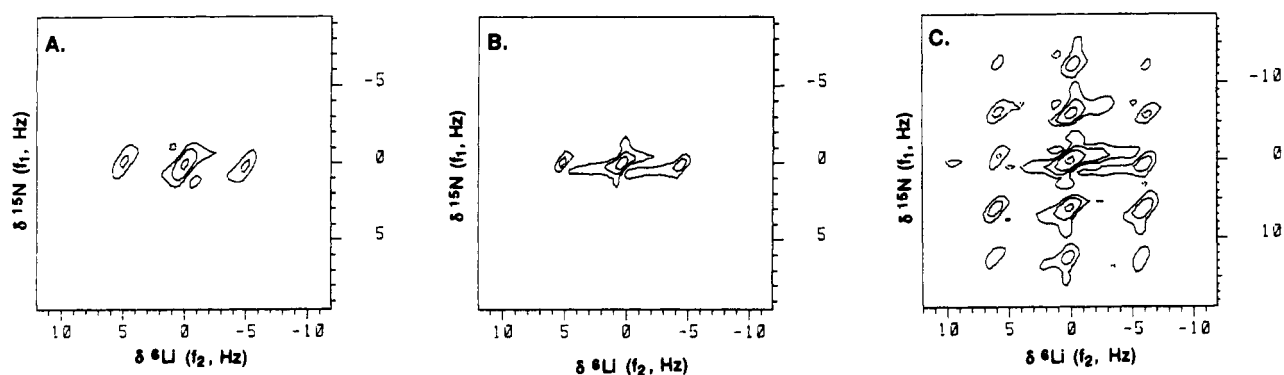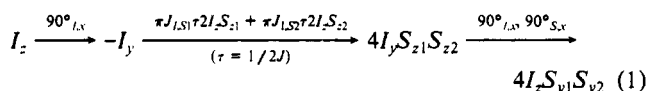

Figure 2. ^{6}Li-detected ^{15}N zero-quantum NMR spectra of (A) 0.15 M [^{6}Li,^{15}N]LDA in THF at -90 °C, (B) 0.10 M [^{6}Li,^{15}N]LiTMP in 3:1 THF/pentane at -115 °C, and (C) 0.25 M [^{6}Li,^{15}N]LiTMP in 3:1 benzene at 30 °C. Spectra were recorded on a Bruker AC 300 spectrometer operating at 44.17 MHz and 30.42 MHz for ^{6}Li and ^{15}N (respectively) with hardware modifications described previously.[2] Data were processed in the phase-sensitive mode. Digital resolution in f_1 prior to zero filling is 2.0 Hz, 1.0 Hz, and 2.4 Hz (respectively) for spectra A–C.

entiates cyclic dimers from higher oligomers of lithium diiso-propylamide (LDA)[5,7] and lithium 2,2,6,6-tetramethylpiperidide (LiTMP).[6]

$$I_z \xrightarrow{90°_{I,x}} -I_y \xrightarrow[(\tau\,=\,1/2J)]{\dfrac{\pi J_{I,S1}\tau 2I_zS_{z1} + \pi J_{I,S2}\tau 2I_zS_{z2}}{}} 4I_yS_{z1}S_{z2} \xrightarrow{90°_{I,x}\,90°_{S,x}}$$
$$4I_zS_{y1}S_{y2} \quad (1)$$

We employed the pulse sequence developed by Müller[14] and Bodenhausen and Ruben[15] for heteronuclear shift correlations (Figure 1). For the phases shown, homonuclear ^{15}N two-spin coherence (a mixture of zero- and double-quantum coherence) is prepared from the two ^{15}N spins neighboring a ^{6}Li atom in a ^{6}Li–^{15}N doubly labeled lithium dialkylamide cyclic oligomer (eq 1).[16] The precession of the zero-quantum coherence during t_1 is modulated by an effective scalar coupling to adjacent ^{6}Li nuclei.

The effective coupling constant (J_{eff}) is defined[17] as

$$J_{\text{eff}} = \Delta m_{\text{N}1}J_{\text{N}1-\text{Li}} + \Delta m_{\text{N}2}J_{\text{N}2-\text{Li}} = (\pm 1)J_{\text{N}1-\text{Li}} + (\mp)J_{\text{N}2-\text{Li}}$$

where $\Delta m_{\text{N}n}$ is the change in quantum number for the ^{15}N nucleus, n, involved in the coherence, and $J_{\text{N}n-\text{Li}}$ is the scalar coupling constant[18] between the ^{6}Li nucleus and ^{15}N$_n$. A ^{6}Li spin coupled equally to ^{15}N$_1$ and ^{15}N$_2$ does not cause splitting of the zero-quantum line in the f_1 (^{15}N) dimension ($J_{\text{eff}} = 0$). For ^{6}Li spins coupled to one ^{15}N spin (but not both), $J_{\text{eff}} = \pm J_{\text{N}n-\text{Li}}$. As a consequence, the multiplicity of the zero-quantum line reveals the number of ^{6}Li spins adjacent to (but not shared by) the ^{15}N–^{15}N two-spin system. For a lithium amide dimer, all ^{6}Li spins coupled to ^{15}N spins involved in the two-spin coherence are coupled to *both* ^{15}N spins. The coupling pattern will be a singlet along the f_1 dimension of the two-dimensional spectrum and a 1:–2:1 triplet along the f_2 dimension. In the case of higher cyclic oligomers, there exist two ^{6}Li spins (*Li* in **3**) that are coupled to one ^{15}N spin, but not both. The zero-quantum coherence will develop scalar coupling to the two nonshared ^{6}Li spins, resulting in a 1:2:3:2:1 pattern along the f_1 dimension and a 1:–2:1 pattern along the f_2 dimension.

The results of the experiment as applied to [^{6}Li,^{15}N]LDA[5] and [^{6}Li,^{15}N]LiTMP[6] in tetrahydrofuran (THF) solutions are illustrated in Figure 2 (A and B, respectively). The coupling patterns show that the aggregated forms are cyclic dimers rather than higher oligomers in both cases. The complementary outcome is illustrated by the spectrum of [^{6}Li,^{15}N]LiTMP in benzene (Figure 2C). The ^{6}Li triplet corresponding to the major[19] cyclic oligomer shows a 1:2:3:2:1 splitting pattern along f_1 consistent with a higher oligomer rather than the dimer.

(1) For additional leading references to ^{6}Li–^{15}N double labeling studies of lithium amides and related N-lithiated species, see ref 3.

(2) Gilchrist, J. H.; Harrison, A. T.; Fuller, D. J.; Collum, D. B. *J. Am. Chem. Soc.* **1990**, *112*, 4069.

(3) Romesberg, F. E.; Gilchrist, J. H.; Harrison, A. T.; Fuller, D. J.; Collum, D. B. *J. Am. Chem. Soc.* **1991**, *113*, 5751.

(4) Galiano-Roth, A. S.; Michaelides, E. M.; Collum, D. B. *J. Am. Chem. Soc.* **1988**, *110*, 2658. Jackman, L. M.; Scarmoutzos, L. M. *J. Am. Chem. Soc.* **1987**, *109*, 5348. Gregory, K.; Bremer, M.; Bauer, W.; Schleyer, P. v. R.; Lorenzen, M. P.; Kopf, J.; Weiss, E. *Organometallics* **1990**, *9*, 1485.

(5) Kim, Y.-J.; Bernstein, M. P.; Galiano-Roth, A. S.; Romesberg, F. E.; Williard, P. G.; Fuller, D. J.; Harrison, A. T.; Collum, D. B. *J. Org. Chem.* **1991**, *56*, 4435.

(6) Hall, P. L.; Gilchrist, J. H.; Harrison, A. T.; Fuller, D. J.; Collum, D. B. *J. Am. Chem. Soc.* **1991**, *113*, 9575. Hall, P. L.; Gilchrist, J. H.; Collum, D. B. *J. Am. Chem. Soc.* **1991**, *113*, 9571.

(7) Galiano-Roth, A. S.; Collum, D. B. *J. Am. Chem. Soc.* **1989**, *111*, 6772. Bernstein, M. P.; Romesberg, F. E.; Fuller, D. J.; Harrison, A. T.; Collum, D. B.; Liu, Q.-Y.; Williard, P. G., submitted for publication.

(8) For extensive reviews of the structures of N-lithiated species, see: Mulvey, R. E. *Chem. Soc. Rev.* **1991**, *20*, 167. Gregory, K.; Schleyer, P. v. R.; Snaith, R. *Adv. Organomet. Chem.*, in press.

(9) Armstrong, D. R.; Barr, D.; Snaith, R.; Clegg, W.; Mulvey, R. E.; Wade, K.; Reed, D. *J. Chem. Soc., Dalton Trans.* **1987**, 1071. Barr, D.; Snaith, R.; Clegg, W.; Mulvey, R. E.; Wade, K. *J. Chem. Soc., Dalton Trans.* **1987**, 2141. Armstrong, D. R.; Mulvey, R. E.; Walker, G. T.; Barr, D.; Snaith, R.; Clegg, W.; Reed, D. *J. Chem. Soc., Dalton Trans.* **1988**, 617.

(10) Newcomb, M.; Varick, T. R.; Goh, S.-H. *J. Am. Chem. Soc.* **1990**, *112*, 5186.

(11) Sapse, A.-M.; Raghavachari, K.; Schleyer, P. v. R.; Kaufmann, E. *J. Am. Chem. Soc.* **1985**, *107*, 6483.

(12) Romesberg, F. E.; Collum, D. B. *J. Am. Chem. Soc.*, in press.

(13) Chandrakumar, N.; Subramanian, S. *Modern Techniques in High-Resolution FT-NMR*; Springer-Verlag: New York, 1987; Chapter 5. Minoretti, A.; Aue, W. P.; Reinhold, M.; Ernst, R. R. *J. Magn. Reson.* **1980**, *40*, 175.

(14) Müller, L. *J. Am. Chem. Soc.* **1979**, *101*, 4481.

(15) Bodenhausen, G.; Ruben, D. J. *Chem. Phys. Lett.* **1980**, *69*, 185.

(16) ^{6}Li and ^{15}N are spin 1 and $^1/_2$ nuclei, respectively.

(17) Sørensen, O. W.; Eich, G. W.; Levitt, M. H.; Bodenhausen, G.; Ernst, R. R. *Prog. Nucl. Magn. Reson. Spectrosc.* **1983**, *16*, 163.

Registry No. LDA, 4111-54-0; LDA cyclic dimer, 137668-29-2; LiTMP, 38227-87-1; LiTMP cyclic dimer, 137003-53-3.

(18) Three-bond ^{15}N–^{6}Li scalar coupling has not been observed.

(19) A minor (approximately 10%) oligomer of LiTMP in benzene is readily observable by standard one-dimensional ^{6}Li and ^{15}N NMR spectroscopy, but is below the lowest contour of Figure 2C.